Two-Dimensional Simulation of the effect of baffles type and number on damping kerosene sloshing in moving tanks

Ahmed Khaled said, Mohamed Ahmed Mohamed
Zagazig university, Egypt, 20812019100122@eng.zu.edu.eg, 20812019100918@eng.zu.edu.eg

Prof. Dr.Ahmed Farouk Abdel Gawad
Prof. Dr.Mofreh Melad Nassief

Zagazig university, Egypt, afaroukgb@gmail.com

Zagazig university, Egypt, mofreh_melad@yahoo.com

Abstract– The studying of sloshing is very important because it has widespread applications in many industries such as automotive, ship building, and aerospace. The load experienced by the tank because of sloshing causes great structural stresses that may lead to a great damage. Sloshing occurs in all types of vehicles that undergo sudden accelerated or decelerated motion.

The effect of baffle types and its number in reducing sloshing effect is investigated in this study. The study includes CFD simulation using ANSYS fluent on two types of baffles: ring and alternating at deferent tank levels. The volume of fluid (VOF) method was used to track the free surface of sloshing in a circular-cylindrical storage tank (tanker) due to sudden changes in braking.

The study shows that the more the number of baffles the lower the force on the tank walls except some cases. The study also shows that ring baffles are preferred in some cases and in other ones alternating baffles are preferred.

Keywords—sloshing- baffles- ANSYS fluent- volume of fluid (VOF) - braking.

I. INTRODUCTION.

Sloshing phenomenon is considered one of the important factors in the design of the liquid storage tanks that transfer fuels and liquids either marine tankers or land tankers.

Sloshing occurs in all types of vehicles that undergo sudden accelerated or decelerated motion. sloshing refers to the periodic motion of the free surface of liquid in a partially filled tank. some fuel large tanks contain fuels in so large quantities that the large fuel motion generates acute hydrodynamic forces that causes instabilities and breakdown of the structure and affects the stability of vehicle carrying the fuel resulting in serious hazards. Resonance also happens either when the external forcing frequency is close to the natural frequency of the liquid or when the frequency of the sloshing waves frequency is close to the frequency of tank material or any material on the vehicle. Therefore, liquid sloshing is a realistic problem related to the safety of the transportation systems, such as liquid tank cars, oil tankers on highways, ships carrying liquid cargo, the liquid tanks used in satellites and spacecrafts.

For the great importance of sloshing, sloshing waves have been studied for several decades. Ling Hou et al [1] have studied numerically the liquid sloshing of a 2-D tank under single excitation and multiple excitations using ANSYS-FLUENT software and the volume of fluid method (VOF). Vaibhav signal [2] have made a CFD analysis of a kerosene fuel tank to reduce liquid sloshing using ANSYS-FLUENT software and the volume of fluid method (VOF). In their simulation they have studied the effect of baffles on making the pick-up pipe completely submerged within the liquid fuel present in the tank. Zhiguo Zhang et al [3] have studied water sloshing in a 2-D rectangular tank using volume of fluid method (VOF) and the time histories of the free surface shape and the dynamic pressure inside the tank are obtained. Nikita Tryaskin et al [4] have studied the sloshing phenomenon in a prismatic membrane – type LNG tank after impact with ice barrier at different speeds and different fillings of tank using opensource code Open FOAM. Abbas Maleki et al [5] have studied the potential of baffles in increasing the hydrodynamic damping of sloshing in a circular – cylindrical storage tanks. Buzhinskii[6] has studied the damping the sloshing in tanks with sharp-edged baffles. Popov et al [7] have studied liquid sloshing in compartmented and baffled rectangular road containers for uniform braking.

In this work, the CFD method is used to make a 2-D simulation on the middle section of a circular-cylindrical tank of a land tanker that transfer Kerosene, this tank is subjected to a sudden change in acceleration (braking). the excitation is given through an acceleration conditional expression. The volume of fluid method is used to track the liquid free surface. This study includes studying of the sloshing in the tank with no baffles and two different types of baffles at different filling levels and investigating the effect of baffles number on damping hydrodynamic forces.

II. COMPUTATIONAL STUDY.

A. *Study description.*

This study investigates the effect of two baffle types on damping kerosene sloshing in a 2D middle section of a circular-cylindrical tank of a land tanker. The first type is the ring baffle and another one is the alternating baffle with different baffle number 2, 4, 8 baffles at different levels as shown in Fig 1, 2, 3.

B. *External excitation.*

In this study, the land tanker travels at constant speed of 80 km/hr, then suddenly brakes and travels with a uniform deceleration of 10 m/s2 until its speed reaches zero within 2.2222 seconds. This motion has been defined for the program using conditional acceleration expressions.

$$IF(t <= 2.222[s], 10\left[{}^{m}/_{s^2}\right], 0\left[{}^{m}/_{s^2}\right])$$

C. *Geometrical model.*

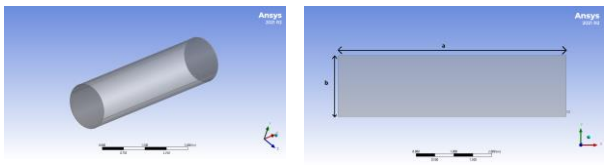

Fig. 1 tank with no baffles.

Fig. 2 tank with ring baffles.

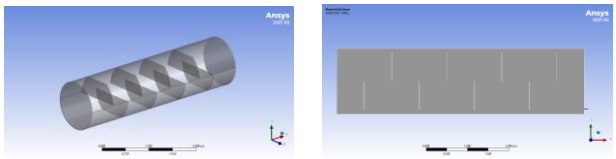

Fig. 3 tank with alternating baffles.

TABLE I
GEOMETRY DIMENSIONS

Dimension	length
a	6 m
b	1.6 m
c	0.5 m
Baffle thick	5 mm

other geometries are the same but with different number of baffles.

C. *Mesh.*

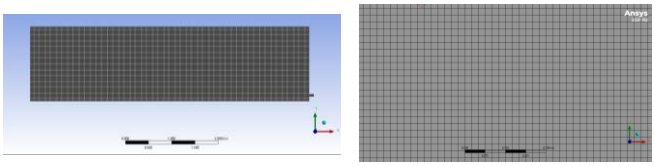

Fig. 4 tank with no baffles mesh.

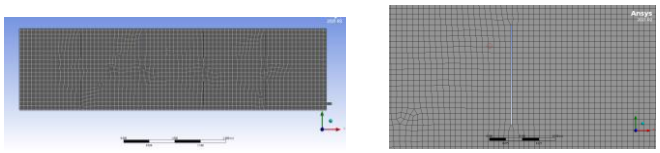

Fig. 5 tank with ring baffles mesh.

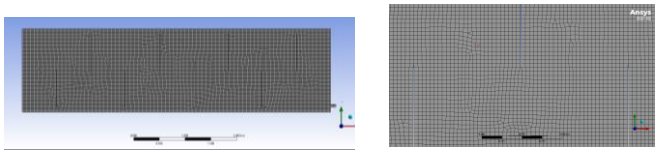

Fig. 6 tank with alternating baffles mesh.

TABLE II
MESH PROPERTIES

Fig no.	Mesh size	Elements no.	Nodes no.
Fig 4	0.025	15368	15677
Fig 5	0.025	15384	15829
Fig 6	0.025	15287	15536

The Fig. 4 represents mesh for tank with no baffles. The fig. 5 represents mesh for the tank with 4 ring baffles. The fig. 6 represents mesh for the tank with 4 alternating baffles. Mesh size in all cases is 0.025 m.

III. COMPUTATIONAL MODELING.

A. *Computational model.*

Volume of fluid (VOF) multiphase model in ANSYS FLUENT was used to capture the motion of the kerosene inside the tank when the tank is under decelerated motion. The VOF model is used to capture the position of interface between two or more immiscible fluids (air and Kerosene). The CFD code ANSYS FLUENT was used for all simulations in this work. the (k-omega sst) was used as a viscous model. the pressure-velocity coupling scheme “PISO” algorithm was used because it has neighbor correction that is highly recommended for all transient flow calculations. The convergence criterion is that the residuals for all governing equations are below 1.0e-4. The time step size is 0.001 s. The method used to predict the kerosene liquid free surface was volume of fluid (VOF) which was designed to capture the position of interface between two or more immiscible fluids (air and kerosene). In the first case, the kerosene was assumed to occupy about 40% of the total volume of the tank and in the second case, The kerosene was assumed to occupy about 80%of the total volume of the tank.

TABLE III
PROPERTIES OF KEROSENE

Property	value
density	780 (kg/m^3)
Surface tension	0.026375 (N/m)
viscosity	0.0024 (kg/m. s)
Specific heat	2090 (j/kg.k)

Thermal conductivity	0.149 (watt/m.k)

B. Governing equation.

1. volume fraction equation

$$\left[\frac{\partial}{\partial t}(\alpha_q \rho_q) + \nabla.(\alpha_q \rho_q \vec{v}_q)\right] = \sum_{p=1}^{n}(\dot{m}_{pq} - \dot{m}_{qp}) + S_{\alpha_q} \quad 1$$

$\dot{m}_{qp}$: *is mass transfer from phase q to phase p*

2. Transport equations for the SST k-omega model

$$\frac{\partial}{\partial t}(\rho k) + \frac{\partial}{\partial x_i}(\rho k u_i) = \frac{\partial}{\partial x_j}\left(\Gamma_k \frac{\partial k}{\partial x_j}\right) + \tilde{G}_k - Y_k + S_k \quad 2$$

$$\frac{\partial}{\partial t}(\rho \omega) + \frac{\partial}{\partial x_i}(\rho \omega u_i) = \frac{\partial}{\partial x_j}\left(\Gamma_\omega \frac{\partial \omega}{\partial x_j}\right) + G_\omega - Y_\omega + D_\omega + S_\omega \quad 3$$

$\tilde{G}_k$: represents the generation of turbulence kinetic energy due to mean velocity gradients
G_ω : represents the generation of ω
Γ_ω and Γ_k : represent the effective diffusivity of k and ω
Y_k and Y_ω : represent the dissipation of k and ω due to turbulence
D_ω : represents the cross-diffusion term

3. Momentum equation.

$$\frac{\partial}{\partial t}(\rho \vec{v}) + \nabla.(\rho \vec{v}\vec{v}) = -\nabla p + \nabla.[\mu(\nabla \vec{v} + \nabla \vec{v}^T) + \rho \vec{g} + \vec{F} \quad 4$$

P : static pressure
$\rho \vec{g}$ *and* $\vec{F}$: are the gravitational body force and external body forces
μ :is the molecular viscosity

4. Continuity equation.

$$\frac{\partial p}{\partial t} + \nabla.(\rho \vec{v}) = S_m \quad 5$$

S_m: is the mass added to the continuous phase from the dispersed second phase

All equations

C. Boundary conditions.

The boundaries in the computational domain in the ring baffles case were named tank walls and baffle walls and their boundary conditions is (no slip wall). The boundaries in the computational domain in the alternating baffles case were named tank walls, upper baffles and lower baffles and their boundary conditions is (no slip wall).

IV. Results and Dissection

A. Load cases.

In this work, numerical simulation with 14 load cases listed in table IV

TABLE IV
CASES

case	Baffles type	Kerosene level	No. of baffles
1	----------	40%	-------
2	----------	80%	-------
3	ring	40%	4
4	ring	80%	4
5	ring	40%	8
6	ring	80%	8
7	ring	40%	2
8	ring	80%	2
9	Alternating	40%	4
10	Alternating	80%	4
11	Alternating	40%	8
12	Alternating	80%	8
13	Alternating	40%	2
14	Alternating	80%	2

B. Results.

1. Case 1. (t= 1.701s)

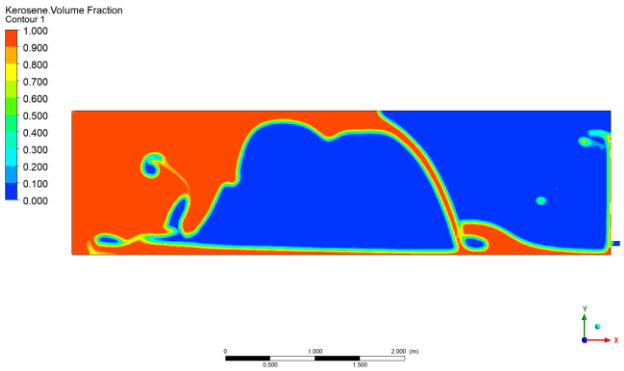

Fig. 7.1 volume of fraction contours.

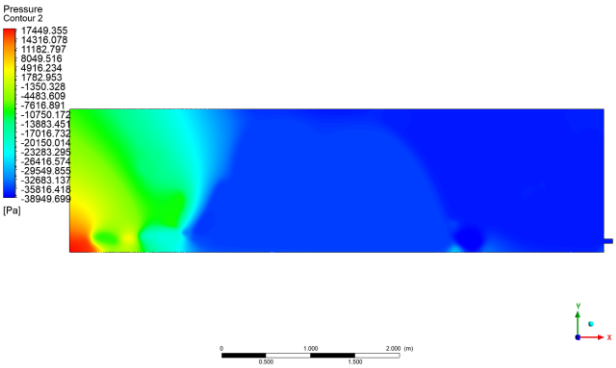

Fig. 7.2 pressure contours.

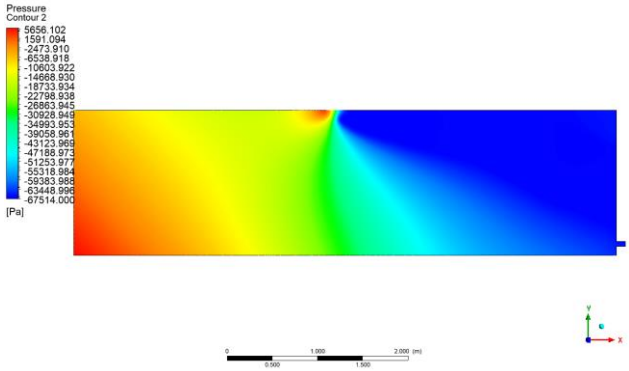

Fig. 8. 2. Pressure contours

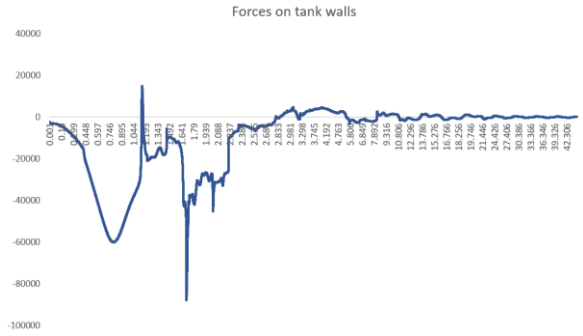

Fig. 7. 3 The force on tank walls.

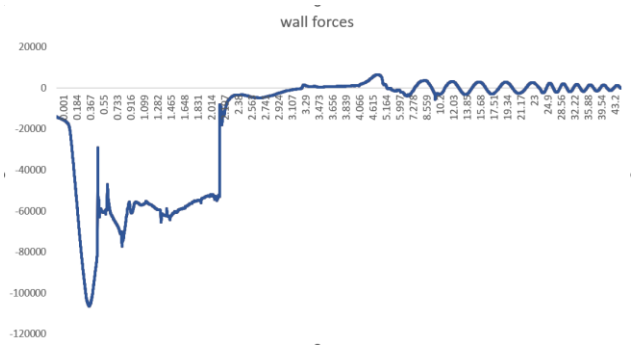

Fig. 8. 3 The force on tank walls

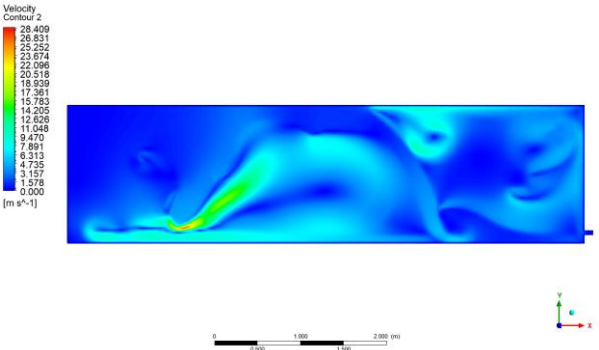

Fig. 7.4 Velocity contours.

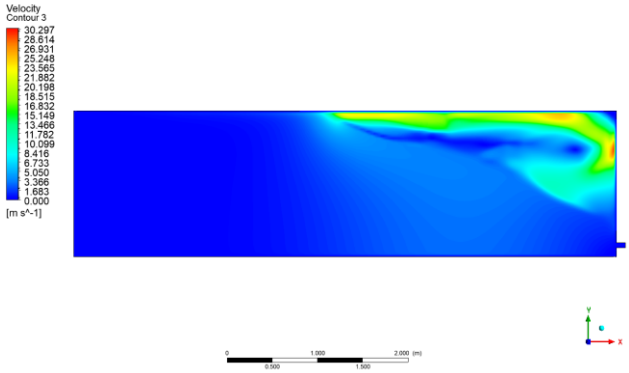

Fig. 8.4 Velocity contours.

2. Case 2. (t= 0.452s)

3. Case 3. (t= 1.369s)

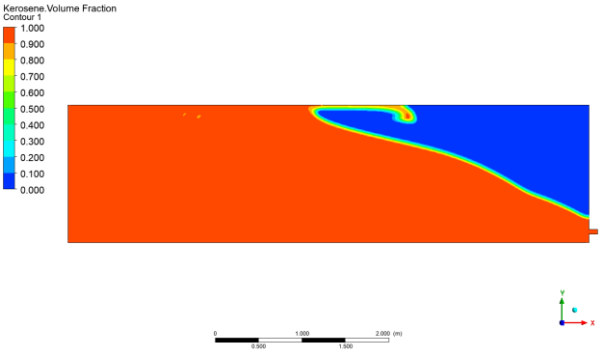

Fig. 8.1 kerosene volume fraction.

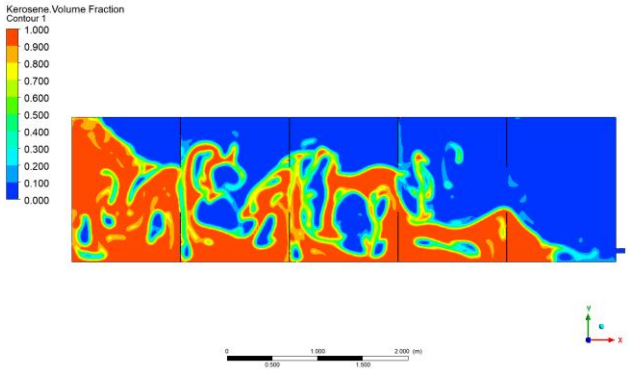

Fig. 9.1 The kerosene volume fraction.

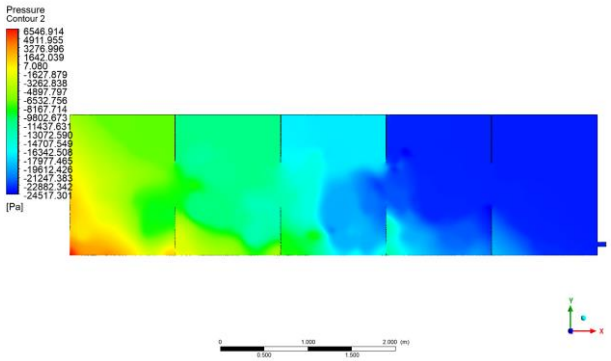

Fig. 9.2. Pressure contours.

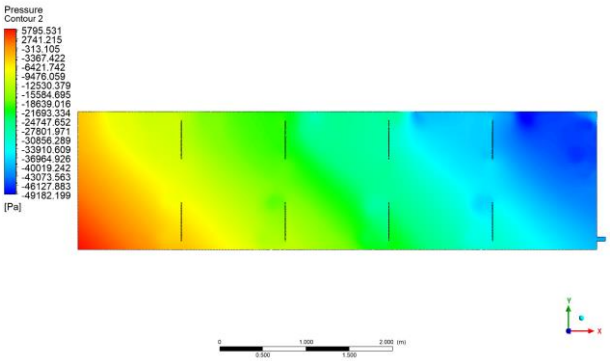

Fig. 10.2 Pressure contours.

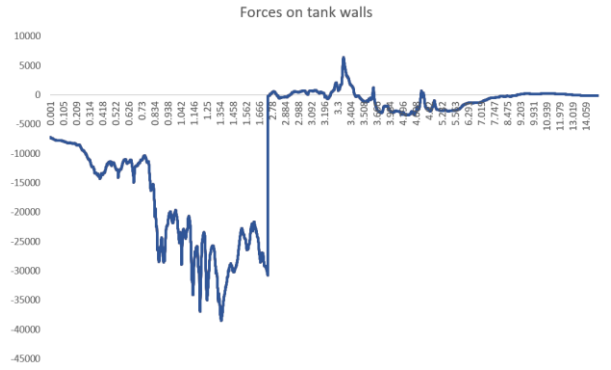

Fig. 9.3 The force on tank walls.

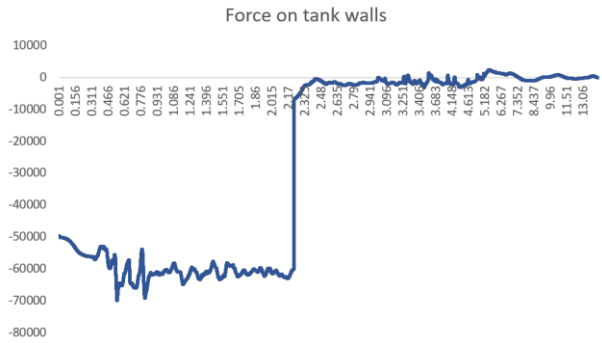

Fig. 10.3 The force on tank walls.

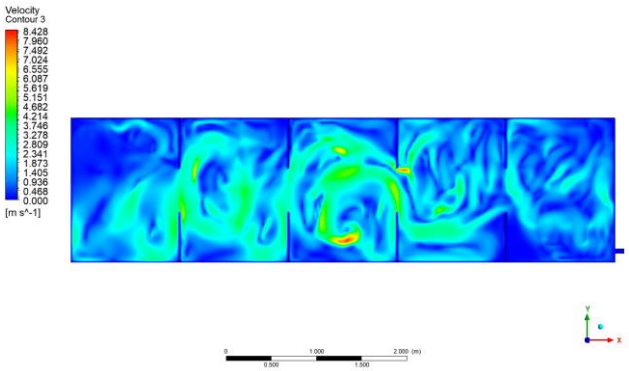

Fig. 9.4 Velocity contours.

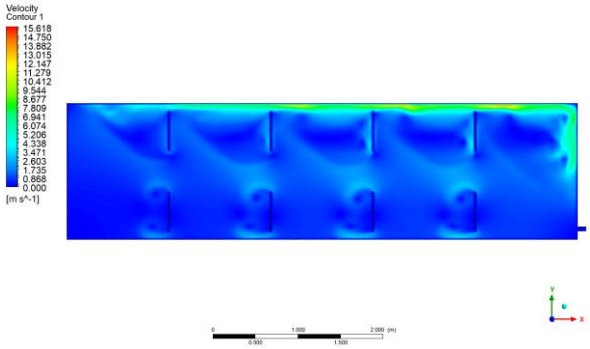

Fig. 10.4 Velocity contours.

4. Case 4. (t= 0.551s)

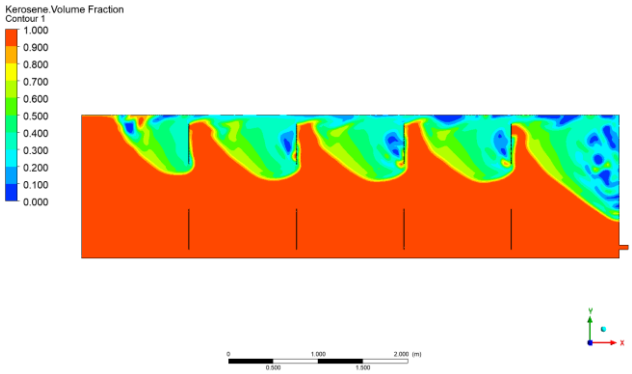

Fig. 10.1 The kerosene volume fraction.

5. Case 5. (t= 1.711s)

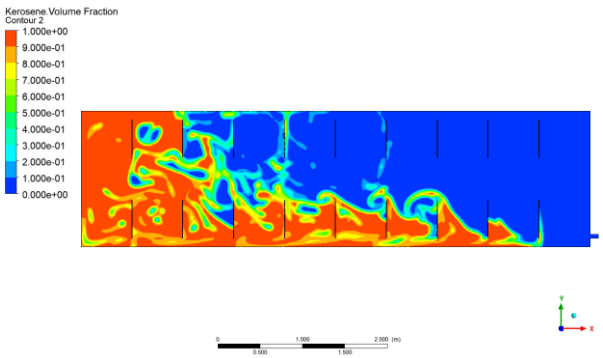

Fig. 11.1 The kerosene volume fraction.

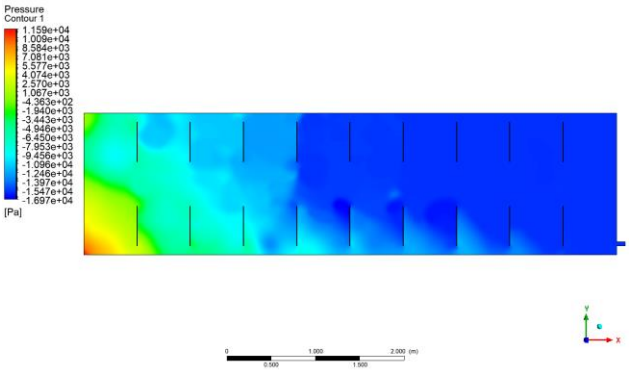

Fig. 11.2 Pressure contours.

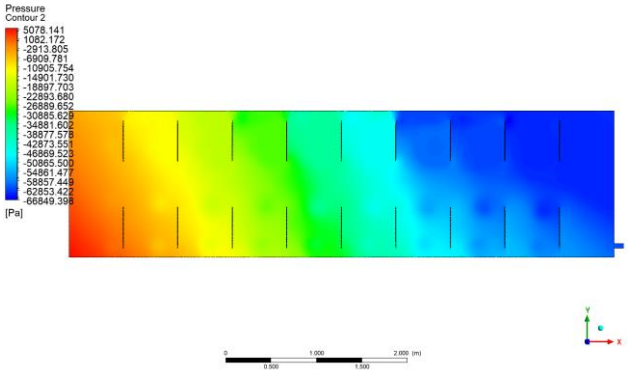

Fig. 12.2 Pressure contours.

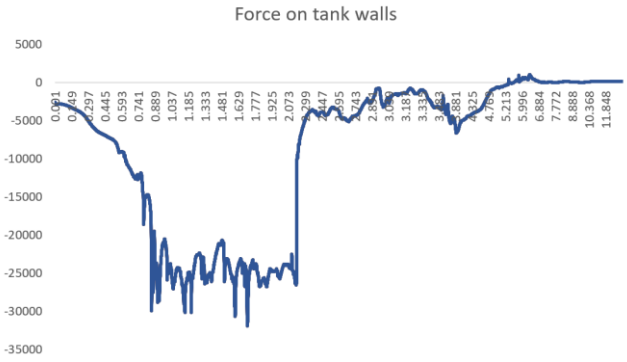

Fig. 11.3 The force on tank walls.

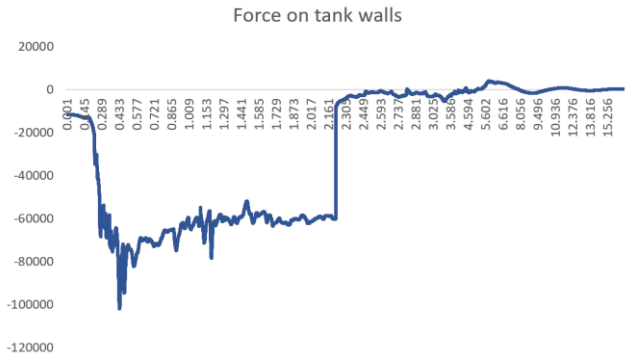

Fig. 12.3 The force on tank walls.

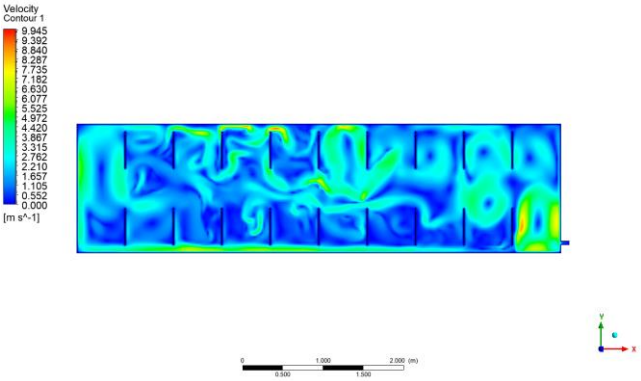

Fig. 11.4 Velocity contours.

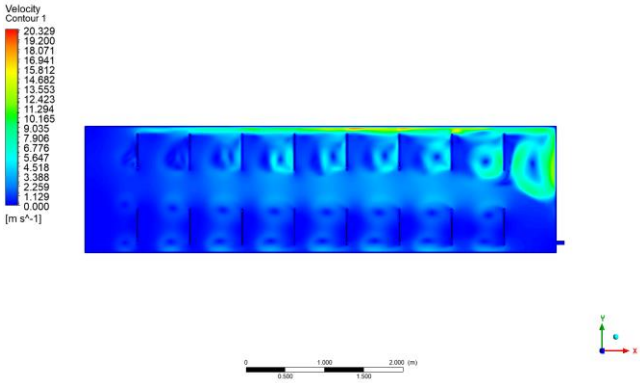

Fig. 12.4 Velocity contours.

6. Case 6. (t= 0.437s)

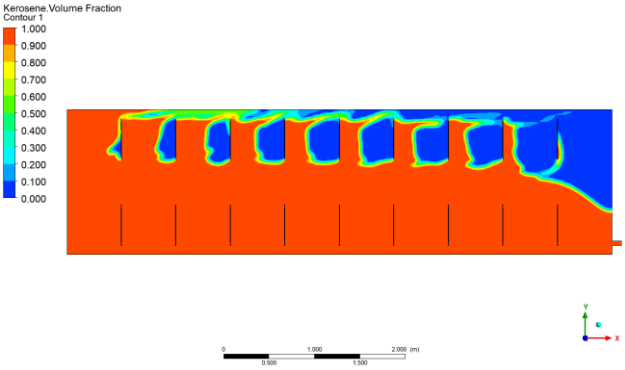

Fig. 12.1 The kerosene volume fraction.

7. Case 7. (t=0.979 s)

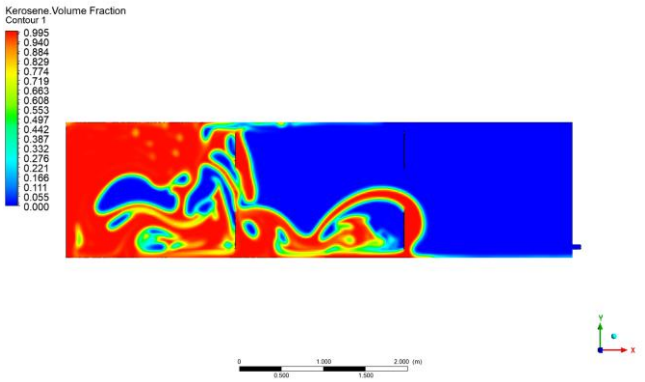

Fig. 13.1 The kerosene volume fraction.

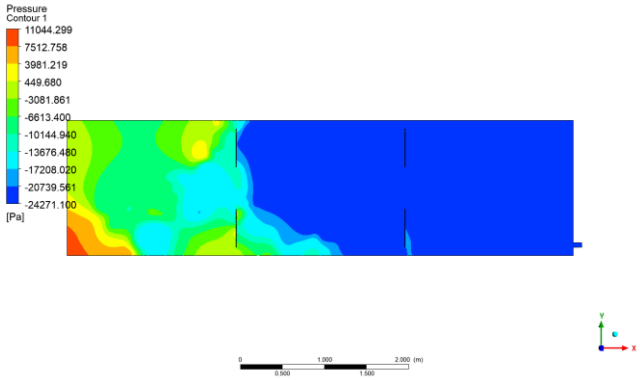

Fig. 13.2 Pressure contours.

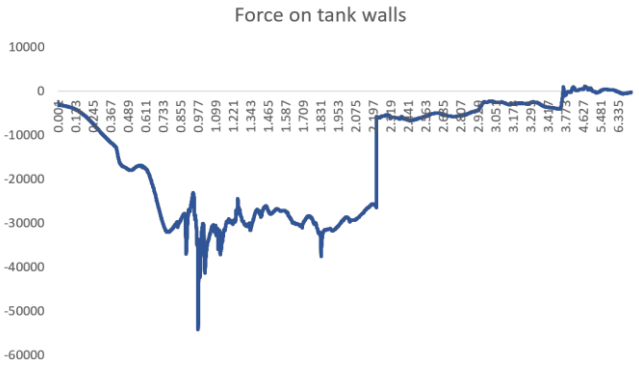

Fig. 13.3 The force on tank walls.

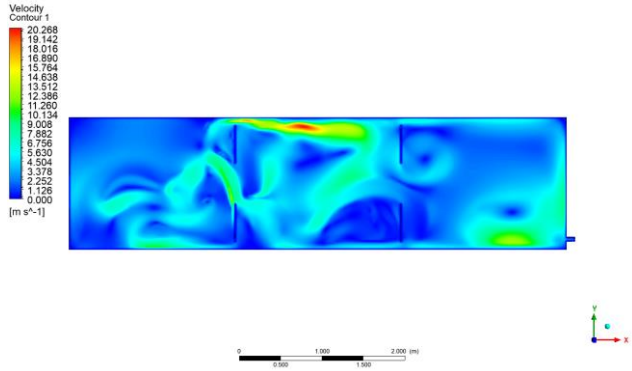

Fig. 13.4 Velocity contours.

8. Case 8. (t= 0.349s)

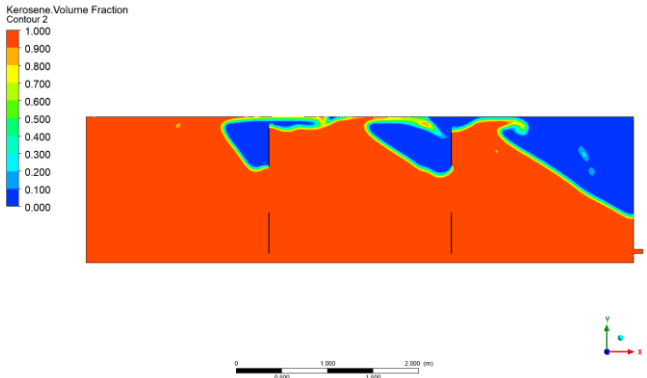

Fig. 14.1 The kerosene volume fraction.

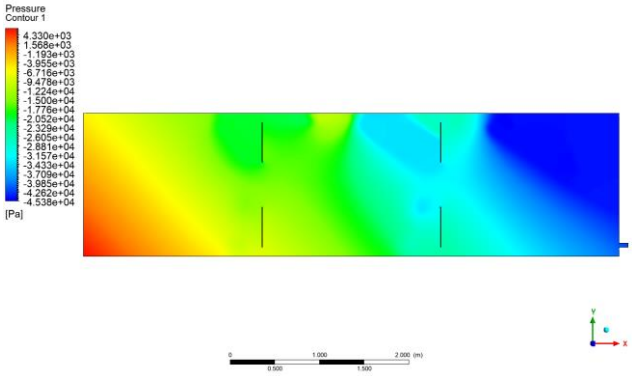

Fig. 14.2 Pressure contours.

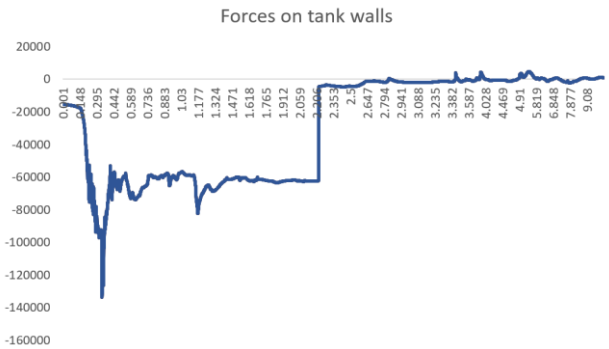

Fig. 14.3 The force on tank walls.

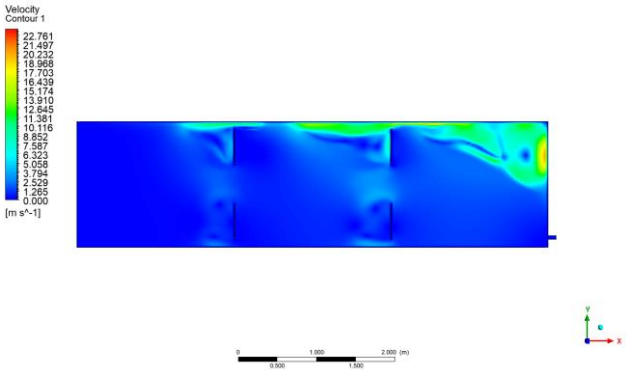

Fig. 14.4 Velocity contours.

9. Case 9. (t= 0.810s)

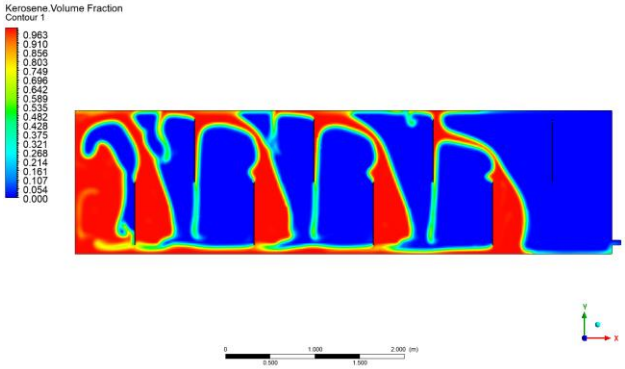

Fig. 15.1 The kerosene volume fraction.

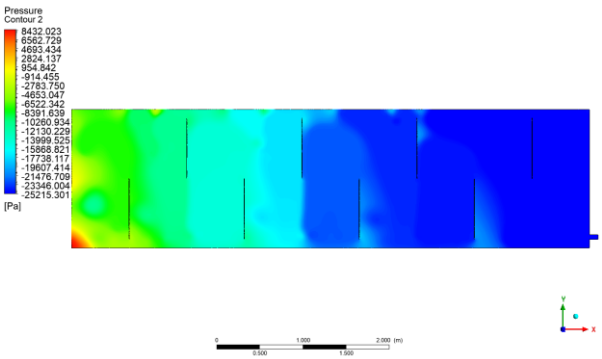

Fig. 15.2 Pressure contours.

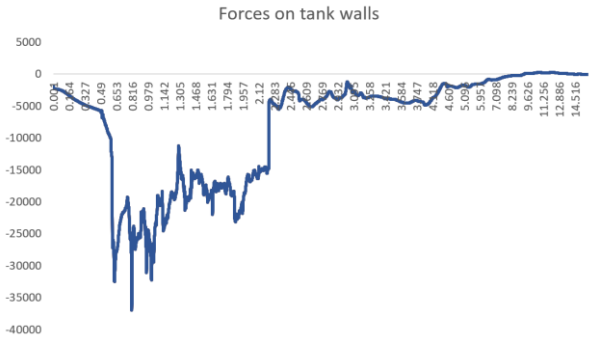

Fig. 15.3 The force on tank walls.

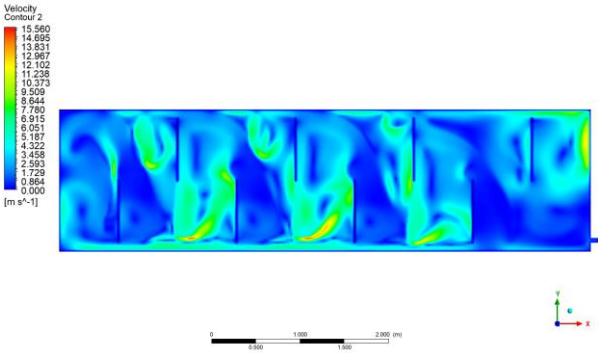

Fig. 15.4: Velocity contour.

10. Case 10. (t= 1.138s)

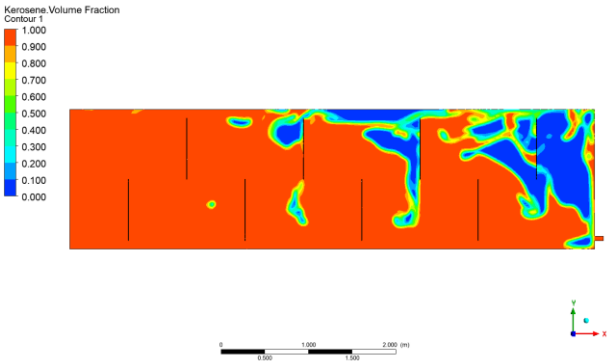

Fig. 16.1 kerosene volume fraction.

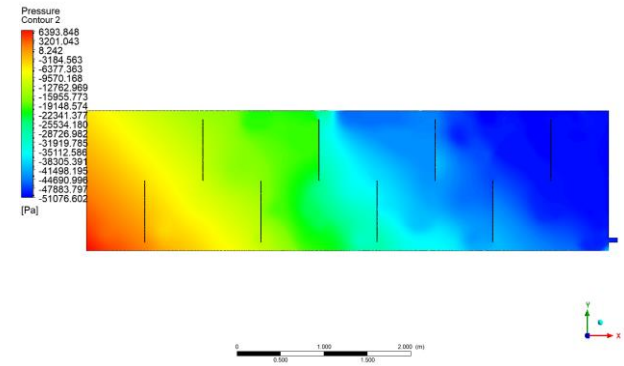

Fig. 16.2 Pressure contours.

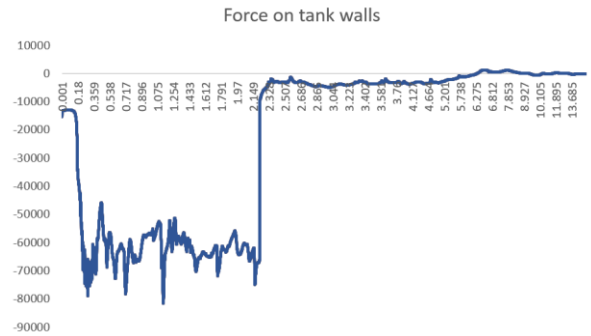

Fig. 16.3 The force on tank walls.

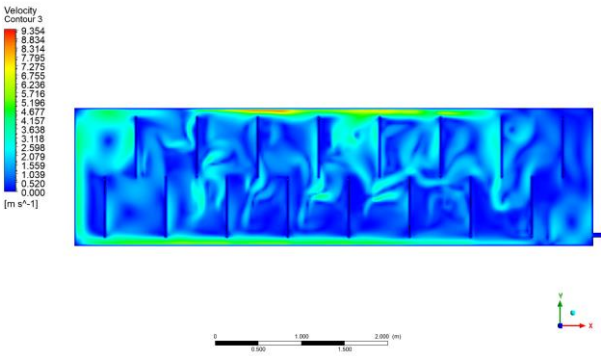

Fig. 16.4. Velocity contours.

11. Case 11. (t= 1.828s)

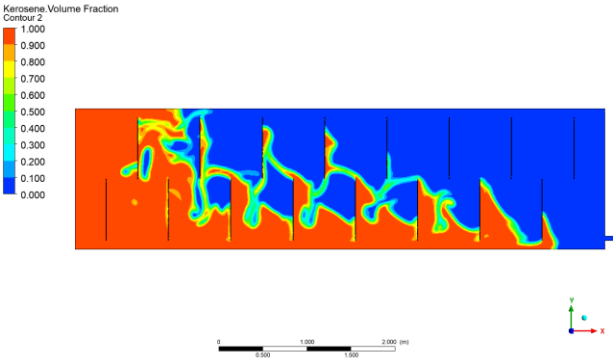

Fig. 17.1 The kerosene volume fraction

.

.

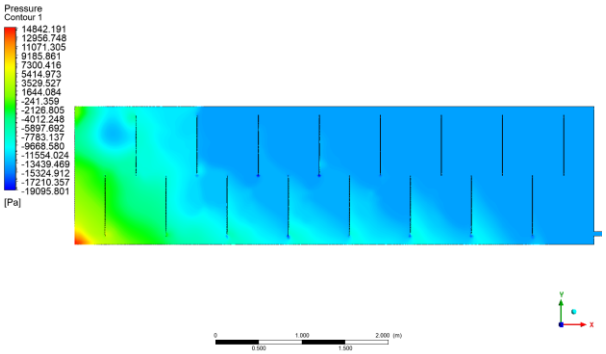

Fig. 17. 2 Pressure contours.

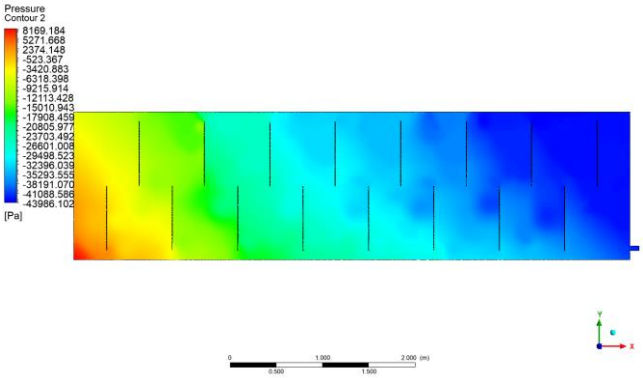

Fig. 18.2 Pressure contours.

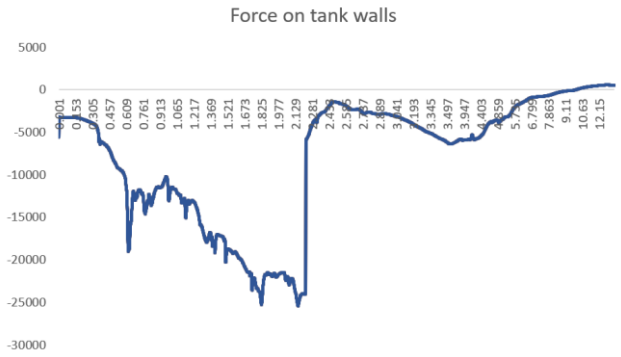

Fig. 17.3 The force on tank walls.

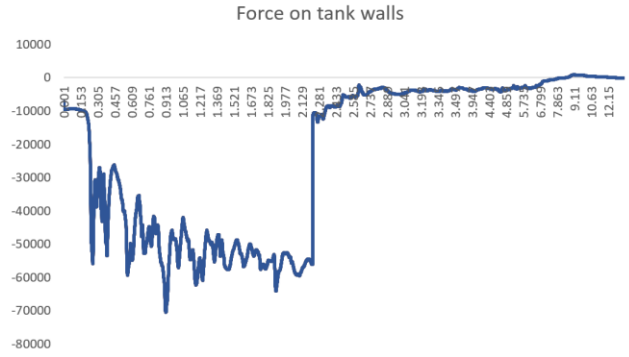

Fig. 18.3: The force on tank walls.

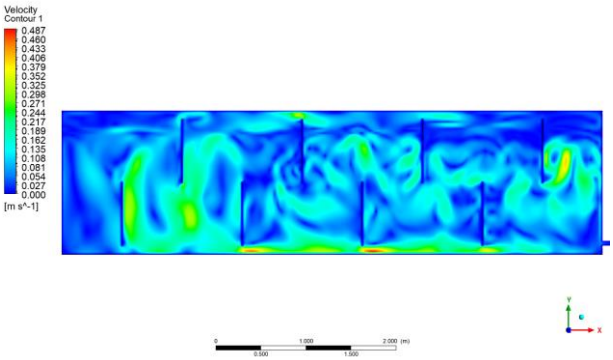

Fig. 17.4. Velocity contours.

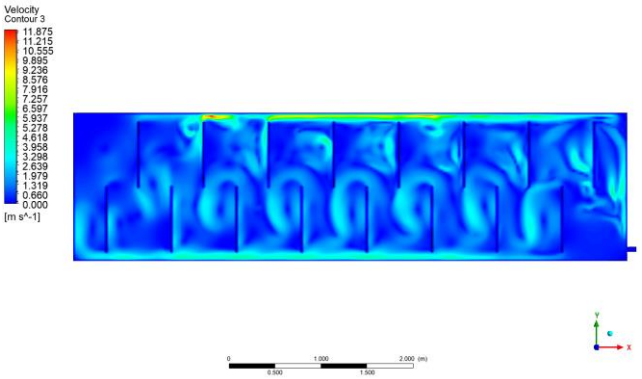

Fig. 18.4 Velocity contours.

12. Case 12. (t= 0.914s)

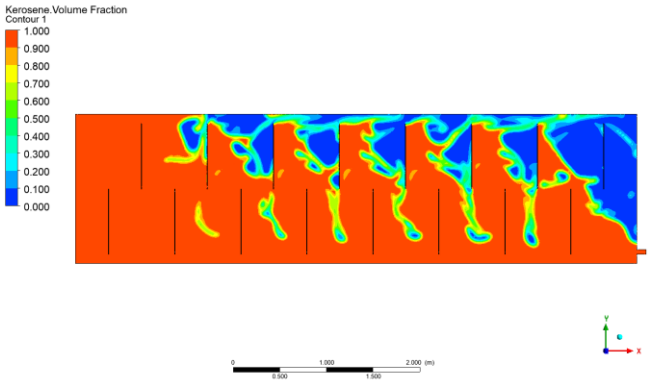

Fig. 18.1 The kerosene volume fraction.

13. Case 13. (t= 0.574s)

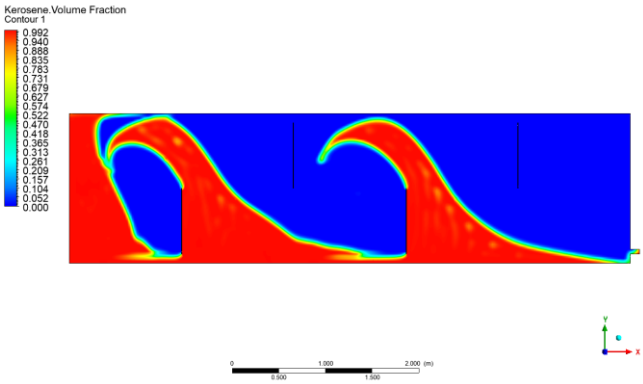

Fig. 19.1 The kerosene volume fraction.

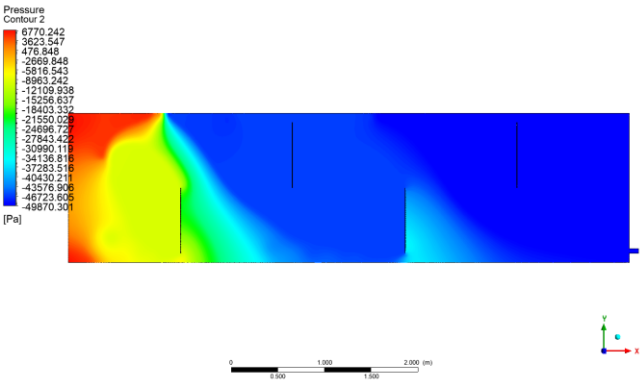

Fig. 19.2 Pressure contours.

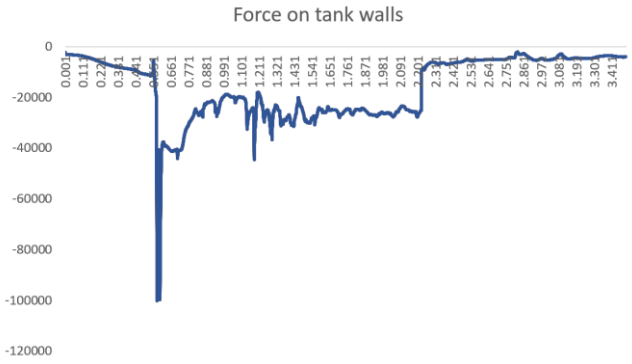

Fig. 19.3 The force on tank walls.

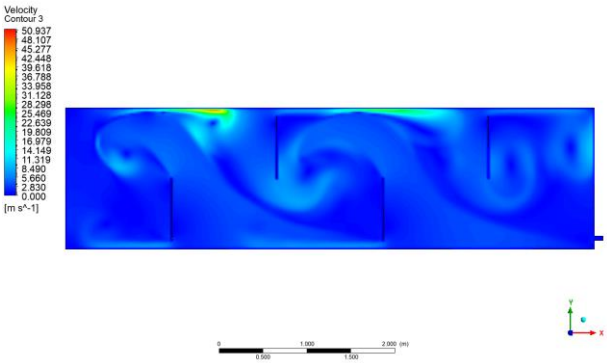

Fig. 19.4 Velocity contours.

14. Case 14. (t= 0.447s)

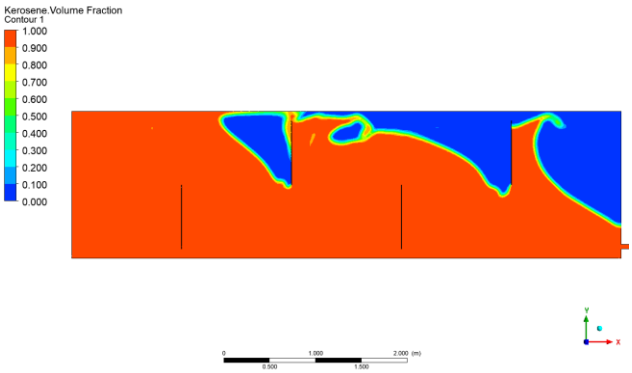

Fig. 20.1 The kerosene volume fraction.

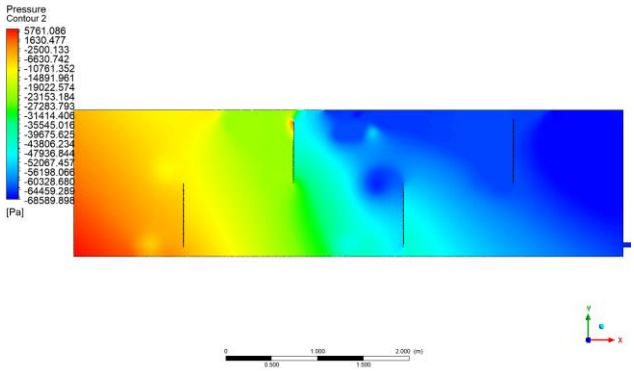

Fig. 20.2 Pressure contours.

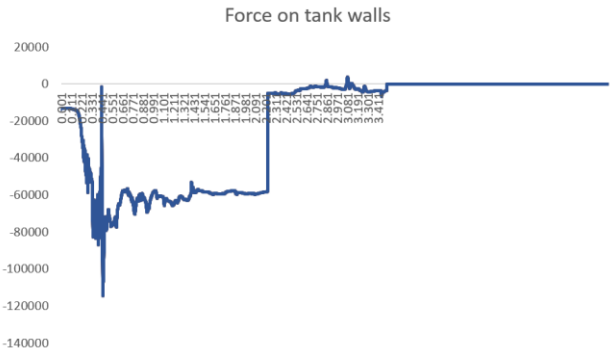

Fig. 20.3 The force on tank walls.

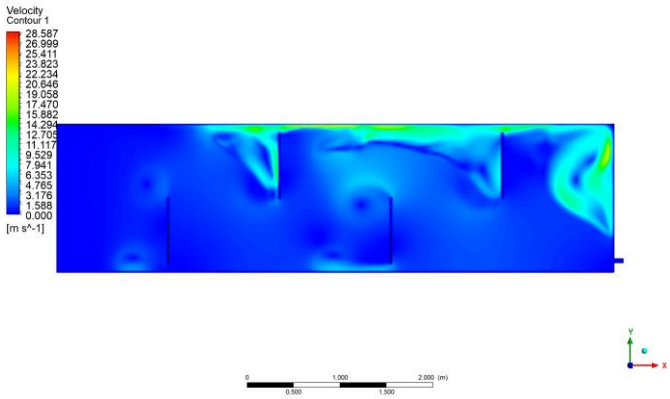

Fig. 20.4. Velocity contours.

C. Discussion.

1. Case 1.

The first graph (Fig. 7.1) shown is for the tank with no baffles and at 40% kerosene level. The graph is at t=1.701 s at which force on tank wall is maximum and equal to 87892.6 N. the second graph (Fig. 7.2) is for the pressure contours at the same time and has a maximum value of 17449.35 pa. the negative pressure is at the right wall and has a maximum value of 38949.92 pa. the time, the force has taken until it comes to zero is 5.8 s. Fig. 7.4 represents velocity contours.

2. Case 2.

The first graph (Fig. 8.1) shown is for the tank with no baffles and at 80% kerosene level. The graph is at t=.452 s at which the force on tank wall is maximum and equal to 106124.055 N. the second graph (Fig. 8.2) is for the pressure contours at the same time and has a maximum value of 8401.266 pa. the negative pressure is at the right wall and has a maximum value of 67740.5 pa. the time, the force has taken until it comes to zero is 10.7 s. Fig. 8.4 represents velocity contours.

3. Case 3.

The first graph (Fig. 9.1) shown is for the tank with 4 baffles and at 40% kerosene level. The graph is at t=1.369 s at which the force on tank wall is maximum and equal to 37865.82 N. the second graph (Fig. 9.2) is for the pressure contours at the same time and has a maximum value of 5795.53 pa. the negative pressure is at the right wall and has a maximum value of 49182.199 pa. the time, the force has taken until it comes to zero is 7.019 s. in this case the force is reduced by 56.9 % from its value at the case of no baffles and the time, the force has taken until it comes to zero is increased by 21 % from its value at the case of no baffles and at the same tank level. Fig. 9.4 represents velocity contours.

4. Case 4.

The first graph (Fig. 10.1) shown is for the tank with 4 ring baffles and at 80% kerosene level. The graph is at t=0.551 s at which the force on tank wall is maximum and equal to 69864.622 N. the second graph (Fig. 10.2) is for the pressure contours at the same time and has a maximum value of 5795.531 pa. the negative pressure is at the right wall and has a maximum value of 49182.199 pa. the time, the force has taken until it comes to zero is 2.48 s. in this case the force is reduced by 34.16 % from its value at the case of no baffles and the time, the force has taken until it comes to zero is reduced by 76.8 % from its value at the case of no baffles and at the Same tank level. Fig. 10.4 represents velocity contours.

5. Case 5.

The first graph (Fig. 11.1) shown is for the tank with 8 ring baffles and at 40% kerosene level. The graph is at t=1.711 s at which the force on tank wall is maximum and equal to 30630.55 N. the second graph (Fig. 11.2) is for the pressure contours at the same time and has a maximum value of 11590 pa. the negative pressure is at the right wall and has a maximum value of 16970 pa. the time, the force has taken until it comes to zero is 5.213 s. in this case the force is reduced by 65.1 % from its value at the case of no baffles and the time, the force has taken until it comes to zero is reduced by 10 % from its value at the case of no baffles and at the same tank level. Fig. 11.4 represents velocity contours.

6. Case 6.

The first graph (Fig. 12.1) shown is for the tank with 8 ring baffles and at 80% kerosene level. The graph is at t=0.437 s at which the force on tank wall is maximum and equal to 101979.58 N. the second graph (Fig 12.2) is for the pressure contours at the same time and has a maximum value of 5078.14 pa. the negative pressure is at the right wall and has a maximum value of 66849.398 pa. the time, the force has taken until it comes to zero is 2.449 s. in this case the force is reduced by 3.9 % from its value at the case of no baffles and the time, the force has taken until it comes to zero is reduced by 77.1 % from its value at the case of no baffles and at the same tank level. Fig. 12.4 represents velocity contours.

7. Case 7.

The first graph (Fig. 13.1) shown is for the tank with 2 alternating baffles and at – kerosene level. The graph is at t=0.979 s at which the force on tank wall is maximum and equal to 54227.12 N. the second graph (Fig. 13.2) is for the pressure contours at the same time and has a maximum value of 10866.834 pa. the negative pressure is at the right wall and has a maximum value of 24271.1 pa. the time, the force has taken until it comes to zero is 3.773 s. in this case the force is reduced by 38.3 % from its value at the case of no baffles and the time, the force has taken until it comes to zero is reduced by 34.9 % from its value at the case of no baffles and at the same tank level. Fig. 13.4 represents velocity contours.

8. Case 8.

The first graph (Fig. 14.1) shown is for the tank with 2 ring baffles and at 80% kerosene level. The graph is at t=.349 s at which the force on tank wall is maximum and equal to 126176.83 N. the second graph (Fig. 14.2) is for the pressure contours at the same time and has a maximum value of 4330 pa. the negative pressure is at the right wall and has a maximum value of 45380 pa. the time, the force has taken until it comes to zero is 2.5 s. in this case the force is increased by 18.9 % from its value at the case of no baffles and the time, the force has taken until it comes to zero is reduced by 76.6 % from its value at the case of no. baffles and at the same tank level. Fig. 14.4 represents velocity contours.

9. Case 9.

The first graph (Fig. 15.1) shown is for the tank with 4 alternating baffles and at 40% kerosene level. The graph is at t=0.81 s at which the force on tank wall is maximum and equal to 36953.11 N. the second graph (Fig. 15.2) is for the pressure contours at the same time

and has a maximum value of 8432.02 pa. the negative pressure is at the right wall and has a maximum value of 25215.301 pa. the time, the force has taken until it comes to zero is 7.098 s. in this case the force is reduced by 57.9 % from its value at the case of no baffles and the time, the force has taken until it comes to zero is increased by 18.2 % from its value at the case of no baffles and at the same tank level. Fig. 15.4 represents velocity contours.

10. Case 10.

The first graph (Fig. 16.1) shown is for the tank with 4 alternating baffles and at 80% kerosene level. The graph is at t=1.138 s at which the force on tank wall is maximum and equal to 81537.54 N. the second graph (Fig. 16.2) is for the pressure contours at the same time and has a maximum value of 6393.848 pa. the negative pressure is at the right wall and has a maximum value of 51076.6 pa. the time, the force has taken until it comes to zero is 5.738 s. in this case the force is reduced by 23.1 % from its value at the case of no baffles and the time, the force has taken until it comes to zero is reduced by 46.3 % from its value at the case of no baffles and at the same tank level. Fig. 16.4 represents velocity contours.

11. Case 11.

The first graph (Fig. 17.1) shown is for the tank with 8 alternating baffles and at 40% kerosene level. The graph is at t=1.828 s at which the force on tank wall is maximum and equal to 24876.6 N. the second graph (Fig. 17.2) is for the pressure contours at the same time and has a maximum value of 14842.19 pa. the negative pressure is at the right wall and has a maximum value of 19095.8 pa. the time, the force has taken until it comes to zero is 9.11 s. in this case the force is reduced by 71.7 % from its value at the case of no baffles and the time, the force has taken until it comes to zero is increased by 36.3 % from its value at the case of no baffles and at the same tank level. Fig. 17.2 represents velocity contours.

12. Case 12.

The first graph (Fig. 18.1) shown is for the tank with 8 alternating baffles and at 80% kerosene level. The graph is at t=0.914 s at which the force on tank wall is maximum and equal to 70563.51 N. the second graph (Fig. 18.2) is for the pressure contours at the same time and has a maximum value of 8169.18 pa. the negative pressure is at the right wall and has a maximum value of 43986.102 pa. the time, the force has taken until it comes to zero is 6.799 s. in this case the force is reduced by 33.5 % from its value at the case of no baffles and the time, the force has taken until it comes to zero is reduced by 36.4 % from its value at the case of no baffles and at the same tank level. Fig. 18.4 represents velocity contours.

13. Case 13.

The first graph (Fig. 19.1) shown is for the tank with 2 alternating baffles and at 40% kerosene level. The graph is at t=0.574 s at which the force on tank wall is maximum and equal to 100080.78 N. the second graph (Fig. 19.2) is for the pressure contours at the same time and has a maximum value of 6770.24 pa. the negative pressure is at the right wall and has a maximum value of 49870.3 pa. the time, the force has taken until it comes to zero is 3.5 s. in this case the force is increased by 12.1% from its value at the case of no baffles and the time, the force has taken until it comes to zero is reduced by 39.6 % from its value at the case of no baffles and at the same tank level. Fig. 19.4 represents velocity contours.

14. Case 14.

The first graph (Fig. 20.1) shown is for the tank with 2 alternating baffles and at 80% kerosene level. The graph is at t=0.447 s at which the force on tank wall is maximum and equal to 114628.394 N. the second graph (Fig. 20.2) is for the pressure contours at the same time and has a maximum value of 5761 pa. the negative pressure is at the right wall and has a maximum value of 68589.89 pa. the time, the force has taken until it comes to zero is 3.411 s. in this case the force is increased by 8% % from its value at the case of no baffles and the time, the force has taken until it comes to zero is reduced by 68.12 % from its value at the case of no baffles and at the same tank level. Fig. 20.4 represents velocity contours.

TABLE V
SUMMARY OF RESULTS

case	Maximum force (N)	Time for zero force	Force reduction%
1	-87892.61	1.701	…….
2	-106124.055	0.452	…….
3	-37865.82	1.369	Reduced by 56.9 %
4	-30630.55	1.711	Reduced by 34.16 %
5	-69864.622	0.551	Reduced by 65.1%
6	-101979.58	0.437	Reduced by 3.9 %
7	-54227.12	0.979	Reduced by 38.3%
8	-126176.83	0.349	Increased by 18.9 %
9	-36953.11	0.810	reduced by 57.9 %
10	-24876.6	1.828	reduced by 23.1 %
11	-81537.54	1.138	reduced by 71.7 %
12	-70563.51	0.914	reduced by 33.5 %
13	-100080.78	0.574	increased by 12.1%
14	-114628.394	0.447	increased by 8%

The relation between the force on tank walls and no. of baffles at different filling levels are illustrated at Fig. 21, 22, 23, and 24.

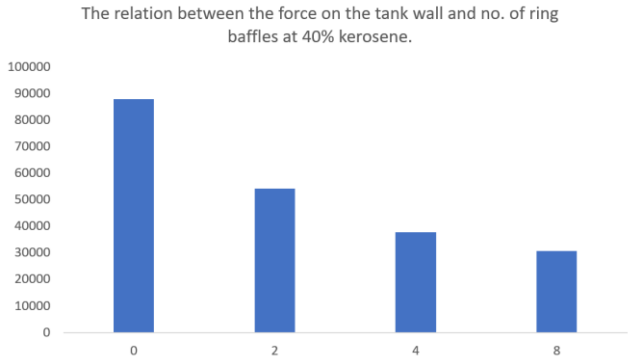

Fig. 21

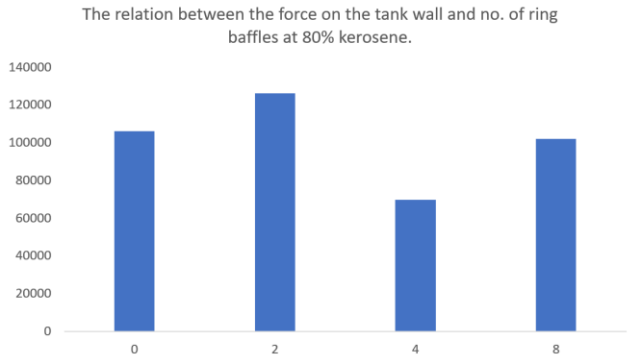

Fig. 22

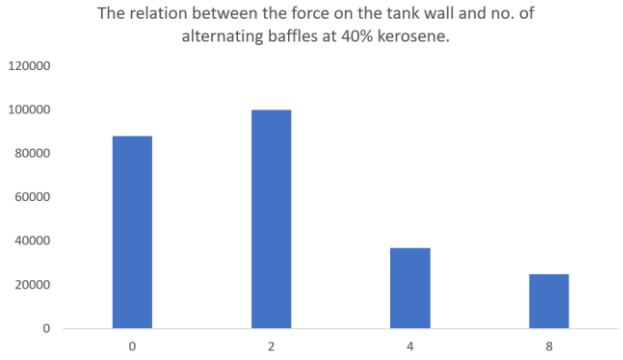

Fig. 23

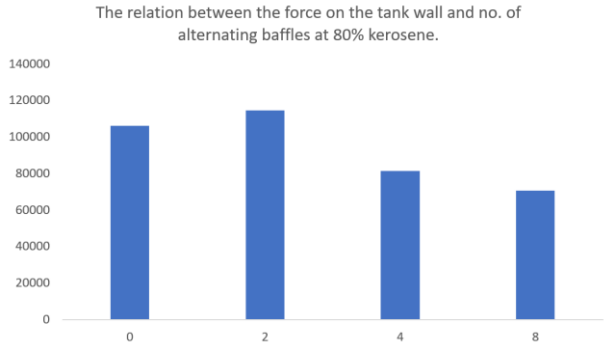

Fig. 24

v. CONCLUSION.

This study investigates the effect of baffle types and numbers on damping kerosene sloshing in a 2-d tank at two different filling levels (40%, 80%). The volume of fluid method was used to predict free surface of the kerosene and the external excitation was in decelerated motion. The study shows that:

- sloshing will be violent in the case of 80% than 40% filling level.
- the difference between the effect of alternating and ring baffles in case of 80% filling level is not large.
- alternating baffles have the largest effect on damping kerosene sloshing in case of 40% filling level
- The study also shows that in the case of two rings or alternating baffles the force increases from its value in case of no baffles except the case of 2 ring baffles at 40% filling level.

ACKNOWLEDGMENT

We would like to convey our thanks to Prof. Dr. Ahmed Farouk Abdel Gawad and Prof. Dr. Moferh Milad for their continuous support in the preparation of the paper. We also would like to convey our thanks to Eng. Ahmed Abdel Salam and Eng. Tarek Elsawy for their tips and their technical support. We also *would like to convey our thanks to* Eng. Eslam Ahmed because he allows us to use his laptop to make simulation.

REFERENCES

[1] H. Ling, L. Fangcheng, and W. Chunliang, "A numerical study of liquid sloshing in a two-dimensional tank under external excitations," *Journal of Marine Science and Application*, vol. 11, no. 3, pp. 305–310, Sep. 2012, doi: 10.1007/s11804-012-1137-y.

[2] S. Vaibhav, B. Jash, A. Nimish, and T. Sarthak, "CFD analysis of a kerosene fuel tank to reduce liquid sloshing," in *Procedia Engineering*, 2014, vol. 69, pp. 1365–1371. doi: 10.1016/j.proeng.2014.03.130.

[3] G. Songqiang, F. Dakui, H. Jing, Z. Zhiguo, and X. Gong, "The numerical simulation of 2D sloshing tank," in *Applied Mechanics and Materials*, 2011, vol. 44–47, pp. 1996–2000. doi: 10.4028/www.scientific.net/AMM.44-47.1996.

[4] T. Nikita and Y. Vladimir, *The proceedings of the twenty-second (2012) International Offshore and Polar Engineering Conference: Rhodes, Greece, June 17-22, 2012*. International Society of Offshore and Polar Engineers, 2012.

[5] M. Abbas and Z. Mansour, "Sloshing damping in cylindrical liquid storage tanks with baffles," *Journal of Sound and Vibration*, vol. 311, no. 1–2, pp. 372–385, Mar. 2008, doi: 10.1016/j.jsv.2007.09.031.

[6] V. A. Buzhinskii, "Vortex damping of sloshing in tanks with baffles," *Journal of Applied Mathematics and Mechanics*, vol. 62, no. 2, pp. 217–224, 1998, doi: 10.1016/S0021-8928(98)00028-8.

[7] G. Popov, S. Sankar, and T. S. Sankar, "Dynamics of Liquid Sloshing in Baffled and Compartmented Road Containers," *Journal of Fluids and Structures*, vol. 7, no. 7, pp. 803–821, Oct. 1993, doi: 10.1006/JFLS.1993.1047.